International Journal of Applied Engineering Research ISSN 0973-4562 Volume 13, Number 10 (2018) pp. 8457-8466

Novel Intelligent Energy Management System for Residential PV Systems in Non-feed-in Tariff Countries

Wilhelm A. Bisschoff, Immanuel N. Jiya and Rupert Gouws

School of Electrical, Electronic and Computer Engineering,
North-West University, Potchefstroom,
South Africa.

Abstract

Currently within South Africa and other developing countries, net-metering policies are not yet widely implemented which hinders the adoption of residential PV systems. Without proper net-metering policies in place, the benefits of residential PV systems are limited to self-consumption as all energy fed into the utility grid is lost without remuneration. This leads to an inefficient and non-profitable PV system. To improve the efficiency and feasibility of the PV system in countries with no feed-in policy, it is of utmost importance that an energy management system (EMS) that optimises self-consumption, of the generated energy, be employed. A new intelligent PV EMS is proposed in this paper which takes historical data of energy consumption and forecasted weather information thereby optimising the energy consumption off the utility grid. Experimental results obtained from a real-world system showed that the local energy consumption percentage increased by 15-20% when compared to a PV system with no EMS.

Keywords: Energy Management, Distributed Generation, PV systems

INTRODUCTION

Rising electricity prices and unreliable supply are driving more residential electricity consumers to installing grid-tied distributed energy resources (DERs) that consist of small scale renewable energy sources such as wind turbines and solar photovoltaic (PV) systems [1], [2] . According to [3] and [4], implementing grid-tied DERs have the ability to drastically improve the reliability of supply whilst decreasing the annual electricity bill. According to [5] achieving the abovementioned requires widespread net-metering policies that permit residential electricity consumers to "sell" excess generated electricity back to distribution utilities.

A statement made by [5] that across the globe, first world and developed countries have these net-metering policies in place; countries such as the Americas, Belgium and Switzerland offers competitive feed-in tariffs which have substantial financial benefits. However, in third world and developing countries these policies are absent [6], [7]. This is owed to safety concerns, a lack of proper electrical infrastructure and poor distribution system management. According to [3] and [4] without proper net-metering policies in place, the benefits of grid-tied DERs are limited to self-consumption as all energy fed into the utility grid is lost without remuneration. This leads to an inefficient and non-profitable DER system. To improve the efficiency and feasibility of the DER system in areas with no feed-in policy, it is of utmost importance that an energy management system (EMS) that optimises self-consumption be implemented.

For the purpose of this study, a novel intelligent EMS was designed for a PV DER. The EMS was implemented as a real-world application by installing a PV system, a grid-tie inverter (GTI), auxiliary relay contacts and the EMS. The residential PV EMS presented in this paper takes historical data of energy consumption and future weather information into account in optimally deciding how energy is consumed by the load. The EMS system controller was a Siemens S7-1200 programmable logic controller (PLC) and was responsible for exercising control over the residential loads. An overview of the integrated system is shown in Figure 1 and explains the interconnection between the main components.

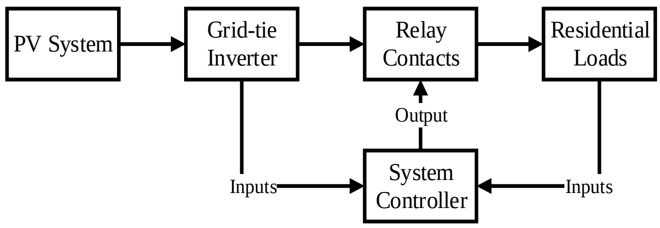

Figure 1. Overview of integrated system

LOAD REQUIREMENTS

The system was specifically designed for the South Africa market and made extensive use of the NRS034-1:2007 standard which describes electricity consumption patterns of different income groups in South Africa, namely living standards measure (LSM). Within the NRS034-1:2007, the electricity demand and consumption profiles of the various income groups were described. Research on the various LSM groups identified which group would most likely adapt a residential PV system and based on these findings, associated residential loads and load profiles were determined. The identified loads that would be controlled were as follows:

- A 150 litre geyser (3 kW)
- A 9 kg washing machine (0.55 kW) and 9 kg tumble dryer (2.2 kW)
- An efficient swimming pool pump (0.6 kW)

- A standard two door refrigerator (0.3 kW)
- A standard dishwashing machine (1.8 kW)

In the study, [8] illustrated that a significant energy consumption reduction was possible by implementing low power LED DC lights. The implementation of DC security lights was therefore included in the design.

DESIGN OVERVIEW

The integrated system was divided into the three sub-systems as illustrated in Figure 2. The first sub-system, namely the energy system, solely consisted of hardware and was responsible for the physical connection between the PV system, GTI, charge controller and loads. The communication and control sub-systems operated alongside each other to manage the hardware as efficiently as possible. The control and communication sub-systems consisted of both hardware and software.

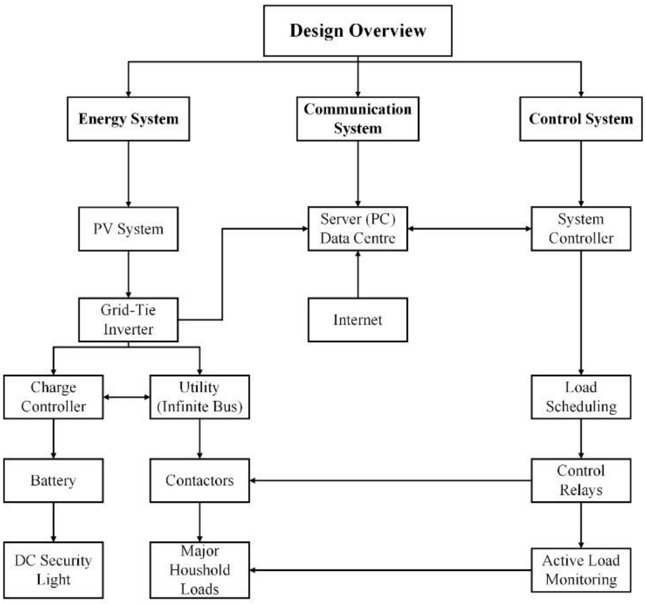

Figure 2. Design overview

A. *Energy System Design*

The energy system was a combination of a DC security light system, PV system, GTI and controllable household loads. As can be seen in Figure 2, the objective of the energy system was to integrate the PV system, battery, GTI and other hardware into a topology that could be integrated with each other and the utility. The PV system was connected via the GTI to the utility grid such that energy generated by the PV system could supply the loads connected in the residence. To actively control the loads in the residence, it was essential that electronically controllable switches, such as contactors relays, were installed in series with the loads that needed to be controlled. By doing so, full control could be exercised over which loads are connected/disconnected to/from the utility and PV system. Figure 3 illustrates the integrated energy system concept along with how the DC security light system fits into the energy system.

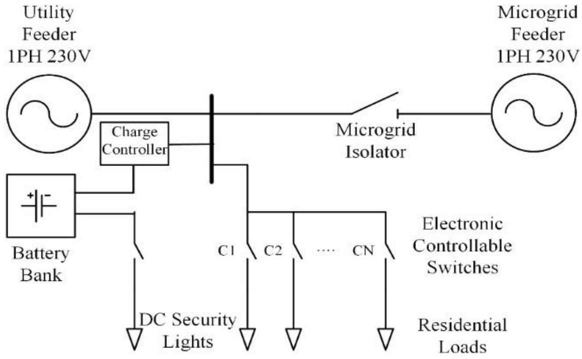

Figure 3. Grid integration and load control

B. *Control System Design*

The control system made use of multiple control strategies which was based on short and long-term inputs. Primarily, for the short-term inputs, the control system ensured that as much as possible of the energy generated by the PV system was consumed locally and power consumption off the grid was minimised. In the case where power generation exceeded power consumption, more loads were switched on to reduce the excess energy. The state-of-charge (SOC) of the battery was also fed to the system controller that aided in the decision-making processes regarding the DC security light system. Long-term inputs included daily expected energy, weather patterns, user priority settings and daily electricity tariff structures. The main purpose of the long-term inputs was to further ensure the optimising of the energy usage within the system. The control system made use of these inputs to schedule the loads according to the expected energy input profile. A summary of the short and long-term inputs that were used are shown in Figure 4.

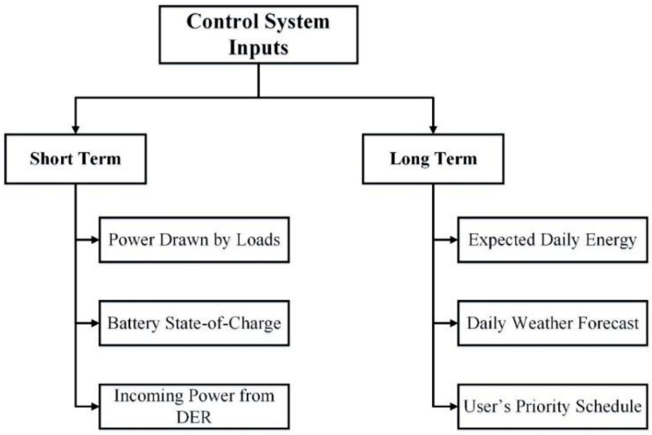

Figure 4. Summary of short and long term inputs to the control system

C. *Communication System Design*

The communication system was used to ensure that short and long-term data are communicated and synchronised across the integrated system network. The short-term control strategy communicated the current drawn by the loads, the battery SOC and incoming power from the PV through the network to a

International Journal of Applied Engineering Research ISSN 0973-4562 Volume 13, Number 10 (2018) pp. 8457-8466

centralised server. This allowed the server to analyse the received measurements, create an energy consumption profile and alter the short-term control strategy to balance incoming power with the power drawn by the loads. Further objectives of the communication system was to obtain weather predictions from an internet RSS feed, accepting user inputs and storing all relevant information in a MySQL database for further analysis. The data was presented in the EMS software interface; the communication system's topology is illustrated in Figure 5.

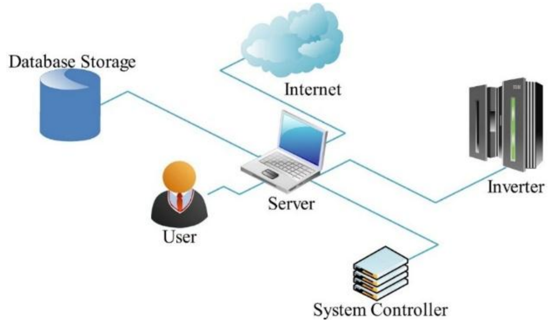

Figure 5. Communication system topology

EXPERIMENTAL TEST STATION

As mentioned in the energy system design section, the system was designed for the South African market and therefore the integrated test station was installed in the town of Potchefstroom in the north-western part of South Africa. The Solar Frontier panels were installed at a residence in Potchefstroom as seen in Figure 6. As seen from Figure 6 the azimuth and tilt of the solar PV panels were directed in a true north orientation at approximately 30˚ inclination. This was in accordance with design recommendations from the PVsyst simulation software.

Figure 6. Installed PV modules

The integrated test station combined all the individual components to create a system where testing could be conducted in a safe and controlled environment. The integrated test station hosted the GTI, contactor relays, system controller and DC security light system. The integrated test station along with the individual components is shown on the left hand side of in Figure 7. On the right hand side of Figure 7, the DC security lights along with the plugs for the loads are shown.

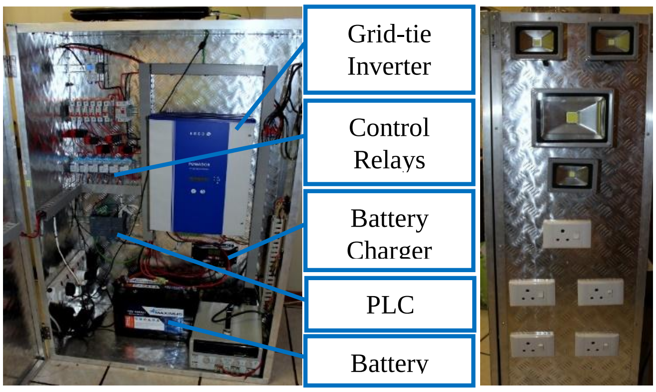

Figure 7. Integrated test station

EMS SOFTWARE INTERFACE

The EMS software interface was divided into four main pages. The first page was the user interface where the user could input the commands to establish the network connection, select the type of day (normal or laundry day) and select the tariff structure. From this page it was also established whether all devices were communicating within the network. On the weather and communication page, the current and predicted weather status was displayed. Apart from the described weather status, graphs visually illustrating the relative humidity, temperature and wind speed were updated in real-time. This data was used to predict the expected daily energy input and optimise the performance of the system. The weather and communication page is shown in Figure 8.

The system dashboard page was designed to provide feedback to the user on the status of the system. Information such as the delivered and consumed energy, maximum power demand and consumption and daily tariff metering were presented on this page. This page was completely autonomous and did not require any inputs from the user. The final page of the EMS software interface was the graphs page which contained real-time graphs of the incoming solar PV power and load status of the testing station. Real-time measurements from the GTI and measurement devices were used to compile these graphs. Also shown on this page was the forecasted solar PV input curve.

Figure 8. EMS software interface

EXPERIMENTAL RESULTS

The experimental results were obtained by allowing the test station to operate for a duration of 34 days. Some of the selected results that were collected were carefully analysed to ensure that no external factors influenced the experimental results. To thoroughly illustrate the operation of the control system, different scenarios are illustrated below. These scenarios have differences relating to the amount of daily input energy and peak power output from the solar PV system and weather conditions such as relative humidity, wind speed and daily temperatures. Each of the scenarios below is discussed according to the input solar PV profile, weather conditions and connected loads.

The EMS was designed according to two scenarios. In the first scenario, the loads that were connected throughout the day included the geyser, swimming pool, battery charger, refrigerator and dishwasher. This scenario was classified as a non-laundry day. The second scenario included the laundry cycle and added the washing machine and tumble dryer to the list of daily loads. The results below are presented according to these two scenarios and are compared to a case where no EMS intervention occurred.

A. EMS Controlled System: Non-Laundry Day

Figure 9 shows the temperature, wind speed and relative humidity throughout the day of testing. It is important to take note that the relative humidity is scaled on the secondary axis of the graph. From Figure 9 it is seen that sunrise and sunset was at 06h48 and 17h24 respectively. The day started out at a relatively low temperature (3˚C), high relative humidity (77%) and no wind. As the day progressed, the temperature rose to a maximum of 20˚C at 13h35. By this time the wind speed increased to 10 km/h which was defined as a light breeze. As the late afternoon set in, the temperature and wind speed gradually declined whilst the relative humidity rose. One of the factors that greatly influenced the amount of incoming solar PV power was the cloud cover index. The captured weather data reported that there was no cloud cover during the day which was indicated as a "Clear" on the weather report.

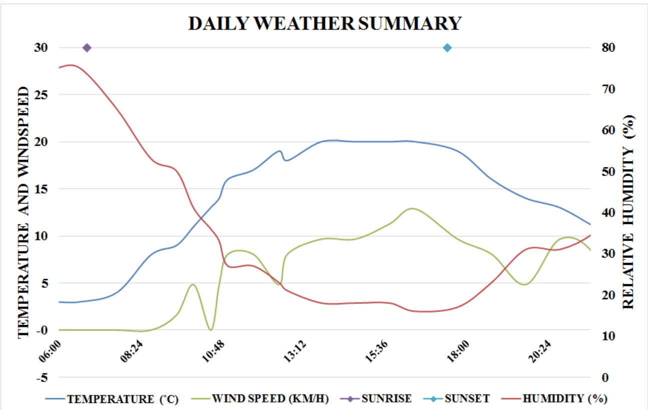

Figure 9. Summary of weather on 9 June 2015

The input solar PV profile and individual load curves corresponding to the weather conditions above are shown in Figure 10. A discussion on the figure follows below where each individual load is addressed accordingly.

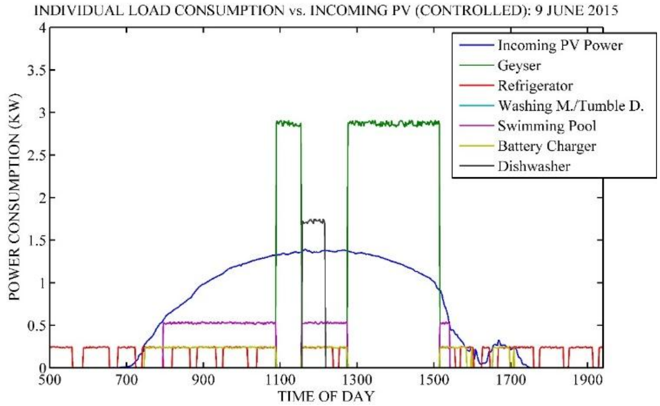

Figure 10. Individual load vs. incoming solar PV plot (9 June 2015)

Incoming PV Power: It is seen that the incoming solar PV power steadily increased to nearly 1.4 kW at noon. The output from the GTI remained steady until 15h15 where a steep drop in the incoming solar PV power was observed. This was due to the fact that a large shadow was cast over a portion of the solar PV panels during the late afternoon. Despite the disrupted solar PV profile due to the shadow, additional performance characteristics of the control system were obtained which are discussed below.

Characteristic	Experimental Result
Total Input Energy	7.81 kWh
Peak Power Output	1.39 kW
Start and Stop Time	07h01 to 17h14
Total Generating Time	10:13 Hours

Geyser: The geyser was switched on at two separate occasions during the day. The first was during the late morning (10h56) hours prior to the dishwasher starting time. This preheated the water for the dishwasher which reduced the runtime of the dishwasher. The second occasion where the geyser was switched on was to heat water for bathing and showering in the evening. The steep drop in the incoming solar PV power during the late afternoon caused the geyser to switch off earlier than expected which led to the water not being heated to the desired temperature. However, the control systems' main objective was to reduce consumption off the utility grid and hence the geyser was switched off when the incoming solar PV power dropped.

Characteristic	Experimental Result
Maximum Power Demand	2.91 kW
Total Run-time	2:58 Hours
Start and Stop Time 1	10h56 to 11h32
Start and Stop Time 2	12h45 to 15h07

International Journal of Applied Engineering Research ISSN 0973-4562 Volume 13, Number 10 (2018) pp. 8457-8466

Refrigerator: As stated previously the refrigerator could not actively be controlled since the compressor operated on its own closed-loop control system. However, control over the refrigerator was exercised by switching off the refrigerator during times when the geyser was switched on. As seen from the curve of the refrigerator, the refrigerator switched on/off spontaneously to regulate the temperature.

Washing Machine/Tumble Dryer: Neither the washing machine or the tumble dryer were switched on in this scenario.

Swimming Pool: The swimming pool pump was switched on during the mid-morning period as soon as the incoming solar PV power exceeded that of 0.55 kW. Whenever sufficient capacity was available, the control system switched on the swimming pool pump. The swimming pool pump was not allowed to be switched on at the same time as the geyser and was therefore switched on at three separate occasions. The steep drop in incoming solar PV power caused the swimming pool pump to switch off to reduce consumption off the utility grid. If the incoming solar PV power did not have such a sharp decrease, the swimming pool pump would have been switched on for another hour. The samples of the load current were taken every 15 seconds and hence the starting and magnetizing currents were not detected. The maximum power demand of the swimming pool pump was 0.54 kW as shown in the table below.

Characteristic	Experimental Result
Maximum Power Demand	0.54 kW
Total Run-time	4:43 Hours
Start and Stop Time 1	07h48 to 10h55
Start and Stop Time 2	11h36 to 12h44
Start and Stop Time 3	15h09 to 15h27

Battery Charger: The battery charger was switched on similarly to the swimming pool i.e. whenever incoming solar PV power exceeded that of 0.25 kW. Whenever this condition was met, the control system switched on the battery charger. In this specific scenario, the battery was almost completely discharged and hence required a longer period of charging. Since the battery was an essential part of the DC security light system that needed to operate during night-time, the battery charger received priority over other loads. This ensured that the battery had adequate charge for the DC security light to operate through the night. Similarly to the geyser and swimming pool pump, its operation was cut short due to the shadow on the solar PV panels. However, upon closer inspection, it was seen that the battery charger was switched on for a fourth time at 16h38 due to increased solar PV power in the late afternoon. The battery charger operating time and SOC (11.62 V) suggested that the battery's initial charge was in the order of 15-25% of the nominal rating.

Characteristic	Experimental Result
Maximum Power Demand	0.25 kW
Total Run-time	5:54 Hours
Start and Stop Time 1	07h10 to 10h55
Start and Stop Time 2	11h36 to 12h44
Start and Stop Time 3	15h09 to 15h57
Start and Stop Time 4	16h38 to 16h51

Dishwasher: The dishwasher was carefully controlled by the control system to switch on during the forecasted peak incoming solar PV power (during noon). It was no different for this scenario and the dishwasher was switched on 24 minutes before noon for 49 minutes. It was expected that the dishwasher would continue for a longer period and hence the geyser starting time was 18 minutes late.

Characteristic	Experimental Result
Maximum Power Demand	1.74 kW
Total Run-time	0:49 Hours
Start and Stop Time 1	11h36 to 12h27

Figure 11 shows the combined load curve versus the incoming solar PV profile. This figure provides insight into how the control system reshaped the load profile according to the available solar PV power. Figure 11 is discussed below according to the annotations made on the figure.

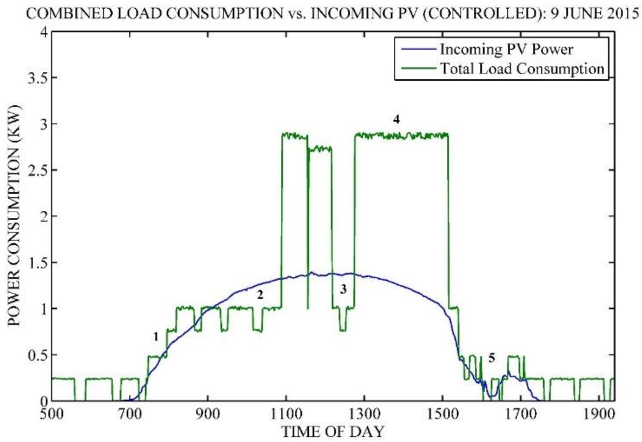

Figure 11. Combined load vs. incoming solar PV plot (9 June 2015)

Note 1: This annotation illustrates that as the incoming solar PV power rose early in the day, the loads were switched on such that the load power consumption grew at the same rate. The instantaneous power consumption was never greater than 1.4 times the incoming solar PV power during this period. This was greater compared to the simulation value of 1.2 times which is owed to the arbitrary switching of the refrigerator.

Note 2 and 3: These annotations illustrated the area where energy was wasted due to the geyser not switching on at exactly the correct time. If the geyser was switched on at roughly 9h30 and 12h15 respectively, the wasted energy would have been minimised.

Note 4: The elimination of loads being simultaneously powered reduced the peak demand to 2.91 kW.

Note 5: The sudden drop in the incoming solar PV power caused the control system to suddenly drop loads. This annotation illustrates that the total load consumption was quickly reduced during this period. As the incoming solar PV power had a late afternoon increase, the control system switched on the battery charger which further charged the battery.

A summary of the experimental results are shown in Table 1. From the table below it is noted that the total daily energy consumption by all the loads were 15.25 kWh. The incoming solar PV power contributed to 46.7% of this total (7.12 kWh). The percentage of incoming solar PV power that was absorbed by the loads (overall system efficiency) was 91.3%.

Table 1. Summary of results (9 June 2015)

Parameter	Result
Total PV Energy Input	7.81 kWh
PV Energy Lost	0.68 kWh
Total Daily Load	15.25 kWh
Energy Cons. off Utility	8.13 kWh
Energy Cons. off PV	7.12 kWh
Percentage Utility Supplied	53.30%
Percentage PV Supplied	46.70%
Maximum Demand	2.91 kW
Overall System Efficiency	91.30%

B. EMS Controlled System: Laundry Day

Figure 12 shows the temperature, wind speed and relative humidity throughout the day of testing. From Figure 12 it is noted that sunrise and sunset was at 06h50 and 17h24 respectively. The day started out at a low to moderate temperature (7˚C), moderate relative humidity (58%) and very little wind. As the day progressed, the temperature gradually rose to a maximum of 17˚C around 15h36. By this time the wind speed increased to 21 km/h which was defined as a moderate breeze. As the late afternoon set in, the temperature and wind speed declined whilst the relative humidity rose. The captured weather data reported that there was no cloud cover during the day which was indicated as a "Clear" on the weather report.

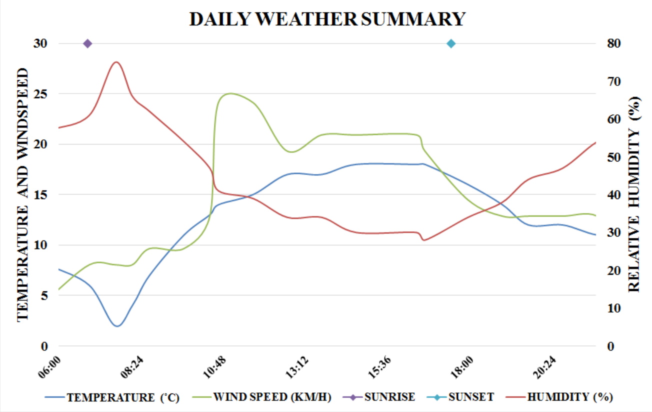

Figure 12. Summary of weather on 10 June 2015

The input solar PV profile and individual load curves corresponding to the weather conditions above are shown in Figure 13. A discussion on the figure follows below where each individual load is addressed accordingly.

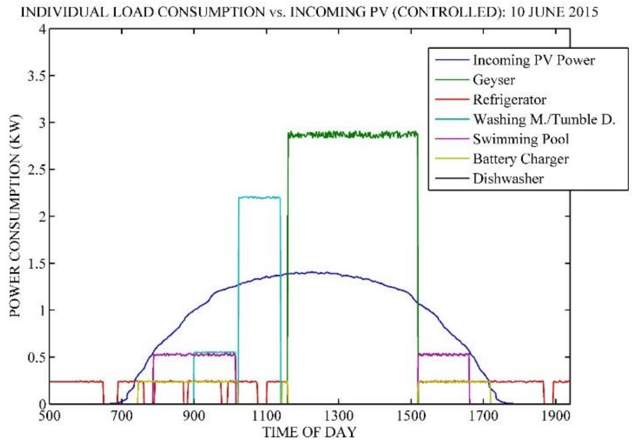

Figure 13. Individual load vs. incoming solar PV plot (10 June 2015)

Incoming PV Power: As seen in Figure 13, there were no disruptions that influenced the incoming solar PV profile. No power fluctuations, shadows or intermittent cloud cover were present in this scenario. The incoming solar PV profile corresponds very well to the weather report yielding satisfactory results. The incoming solar PV power provided a longer than usual day of power generation, stretching from 06h50 to 17h25.

Characteristic	Experimental Result
Total Input Energy	8.81 kWh
Peak Power Output	1.41 kW
Total Generating Time	10:35 Hours
Start and Stop Time	06h50 to 17h25

Geyser: Due to the day being allocated for laundry purposes, the geyser was switched on at only one occasion during the day. This was done prior to noon. The geyser was then switched off at 15h07 to allow the battery charger and swimming pool pump to be switched on. Since the washing machine and tumble dryer was required during the day, there was no time in the morning to switch the geyser on for additional water heating.

Characteristic	Experimental Result
Maximum Power Demand	2.90 kW
Total Run-time	3:22 Hours
Start and Stop Time	11h45 to 15h07

Refrigerator: Control over the refrigerator was exercised by switching off the refrigerator during the times when the geyser was switched on.

Washing Machine/Tumble Dryer: The washing machine and tumble dryer were time of day controlled and set to switch on during the late morning hours when incoming solar PV power was sufficient. The washing machine had a lower power requirement than the tumble dryer and was switched on at 09h00 and finished at 09h55. Thereafter the tumble dryer was switched on which continued to 11h15. During the operation of the tumble dryer all loads except the refrigerator was switched off to minimise consumption off the utility grid.

Characteristic	Experimental Result
Maximum Power Demand	0.56 kW and 2.18 kW
Total Run-time	2:15 Hours
Start and Stop Time 1	09h00 to 09h55
Start and Stop Time 2	09h57 to 11h15

Swimming Pool: The swimming pool pump was switched on as soon as the incoming solar PV power exceeded that of 0.55 kW. This caused that whenever sufficient capacity was available, the control system switched on the swimming pool. The swimming pool was not allowed to be switched on at the same time as the geyser and tumble dryer. The swimming pool was switched on at two separate occasions, 07h48 and 11h36. This resulted in a total operating time of 4:43 hours.

Characteristic	Experimental Result
Maximum Power Demand	0.56 kW
Total Run-time	4:43 Hours
Start and Stop Time 1	07h48 to 10h55
Start and Stop Time 2	11h36 to 12h44

Battery Charger: The battery charger switched on as soon as the incoming solar PV power exceeded that of 0.25 kW. Whenever this condition was met, the control system would switch on the battery charger which allowed charging of the battery to occur. In this specific scenario, the battery charger was switched on at four separate occasions. The first was at 07h10, the second at 11h36, the third at 15h08 and the last at 16h38. The total run-time for the battery charger was 5:54 hours. The 5:54 hours of battery charging ensured that the battery was charged to 95% SOC (12.61 V).

Characteristic	Experimental Result
Maximum Power Demand	0.24 kW
Total Run-time	5:54 Hours
Start and Stop Time 1	07h10 to 10h55
Start and Stop Time 2	11h36 to 12h44
Start and Stop Time 3	15h08 to 15h57
Start and Stop Time 4	16h38 to 16h51

Dishwasher: The dishwasher was not switched on in this scenario due to limited time available to perform the washing and tumble drying tasks.

Figure 14 shows the combined load curve versus the incoming solar PV profile. This figure provides insight into how the control system reshaped the load profile according to the available solar PV power. Figure 14 is discussed below according to the annotations made on the figure.

Note 1 and 4: The incoming solar PV profile was near perfect for the entire day and hence these results were the closest comparable to the simulation results. During the mid-morning period, the incoming solar PV power rose gradually which caused the control system to switch on the battery charger and swimming pool pump as soon as sufficient capacity was available. In a similar manner, the control system switched off the swimming pool and battery charger as the incoming power became less than the respective threshold values.

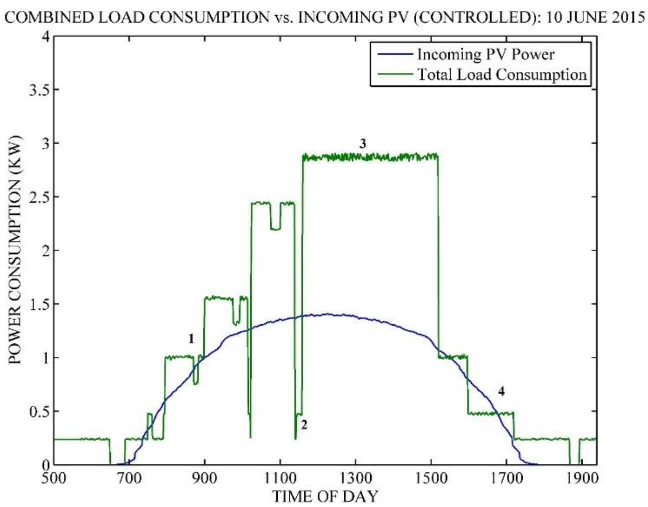

Figure 14. Combined load vs. incoming solar PV plot (10 June 2015)

Note 2: The sudden drop in power consumption was owed to the tumble dryer finishing its operating cycle 9 minutes early. During the tumble dryer's cycle all other loads except the refrigerator were already switched off. This caused the significant drop in consumption when the tumble dryer finished its cycle earlier than expected.

Note 3: The peak demand of the day was set by the geyser at 2.91 kW.

A summary of this scenario's experimental results are shown in Table 2. From the table it is seen that the total daily energy consumption by all the loads were 18.20 kWh with the solar PV supplying 47.75% of this total (8.50 kWh). The percentage of incoming solar PV power that was absorbed by the loads (overall system efficiency) was 96.6%. A satisfactory percentage of the load was covered by the incoming solar PV power and hence only 9.7 kWh was required from the utility.

Table 2: Summary of results (10 June 2015)

Parameter	Result
Total PV Energy Input	8.81 kWh
PV Energy Lost	0.29 kWh
Total Daily Load	18.20 kWh
Energy Cons. off Utility	9.70 kWh
Energy Cons. off PV	8.50 kWh
Percentage Utility Supplied	53.25%
Percentage PV Supplied	46.75%
Maximum Demand	2.91 kW
Overall System Efficiency	96.60%

C. *Uncontrolled System*

To directly compare the uncontrolled to the controlled system experimental results, it was necessary to have a consistent uncontrolled system load profile. The load profile was taken from a normal non-laundry day with accurate timestamps. The timestamps of the discussed solar PV input profiles were matched to the load profile's timestamps and hence accurate calculations could be performed. The individual load curve along with the various solar PV profiles is shown in Figure 15.

Incoming PV Power: The incoming solar PV profiles were discussed in the previous sections and are not discussed in this section.

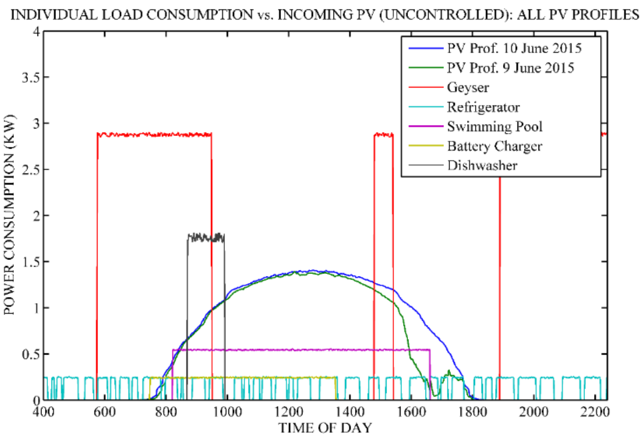

Figure 15. Uncontrolled individual curve

Geyser: The geyser element was switched on at three separate occasions during the day. The first was during the early morning hours (05h50) when the user bathed which caused hot water to flow out of the water tank and had to be replaced by cold water. The second occasion was in the early afternoon and caused the geyser element to be switched on for a short period to maintain the hot water temperature. In the late afternoon, the residents used hot water for cooking and bathing purposes which triggered the geyser element to switch on for a third occasion.

Characteristic	Experimental Result
Maximum Power Demand	2.91 kW
Total Run-time	6:07 Hours
Start and Stop Time 1	05h50 to 07h58
Start and Stop Time 2	14h48 to 15h32
Start and Stop Time 3	19h25 to 22h40

Refrigerator: As can be seen from the curve of the refrigerator, it was switched on/off spontaneously to regulate the temperature inside the refrigerator box.

Washing Machine/Tumble Dryer: Neither the washing machine nor the tumble dryer was switched on in this scenario.

Swimming Pool: The swimming pool pump was switched on at 08h15 and switched off at 16h45.

Characteristic	Experimental Result
Maximum Power Demand	0.54 kW
Total Run-time	8:30 Hours
Start and Stop Time	08h15 to 16h45

Battery Charger: The battery charger switched on as soon as the incoming solar PV power exceeded 0~kW and switched off as soon as the battery was fully charged.

Characteristic	Experimental Result
Maximum Power Demand	0.25 kW
Total Run-time	5:55 Hours
Start and Stop Time	07h40 to 13h35

Dishwasher: The dishwasher was manually switched on at 08h50 and finished its cycle within 1 hour and 5 minutes.

Characteristic	Experimental Result
Maximum Power Demand	1.74 kW
Total Run-time	1:05 Hours
Start and Stop Time	08h50 to 09h55

Figure 16 shows the uncontrolled combined load curve versus the incoming solar PV profile. This figure provides insight into how the load profile was according to the available solar PV power without the control system. Figure 16 is discussed below according to the annotations made on the figure.

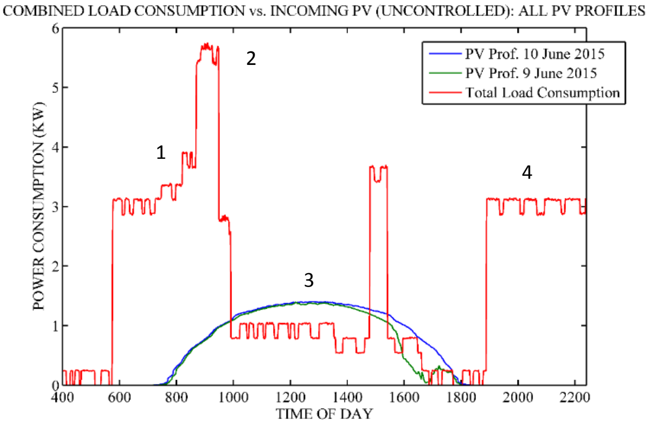

Figure 16. Uncontrolled combined curve

Note 1, 2 and 4: These annotations illustrate that the maximum power demand of 5.75 W was during the mid-morning period (09h00). This was undesirable as there were very little incoming solar PV power during this period. Also during the early evening hours excessive energy consumption occurred.

Note 3: This annotation highlights the fact that during the peak solar PV generation period, the load consumption was less than the solar PV generation. This caused the excess energy to feed into the utility grid and was lost.

From Table 3, a summary of the uncontrolled results compared to the various incoming solar PV profiles are shown. It should be noted that the overall system efficiency was not only dependent on the incoming solar PV power and the load consumption. The overall system efficiency was predominantly influenced by the incoming solar PV profile.

Table 3: Summary of results (Uncontrolled)

Parameter	10 June 2015	9 June 2015
Total PV Energy Input	8.81 kWh	7.81 kWh
PV Energy Lost	2.46 kWh	1.86 kWh
Total Daily Load	34.19 kWh	34.19 kWh
Energy Cons. off Utility	27.83 kWh	28.23 kWh
Energy Cons. off PV	6.35 kWh	5.95 kWh
Percent. Utility Supplied	81.4%	82.6%
Percent. PV Supplied	18.6%	17.4%
Maximum Demand	5.75 kW	5.75 kW
Overall System Eff.	72.1%	76.2%

The experimental results of these scenarios proved that the percentage of the solar PV generated energy absorbed locally ranged from 72.1% to 76.2% when no EMS was implemented. It further showed that the utility grid supplied at least 81.4% of the daily energy requirement on days when the solar PV energy yield was quite high.

The first scenario of the controlled system experimental test (non-laundry day) was conducted when the weather status was classified as "clear skies". A significant improvement was seen compared to the uncontrolled system. The percentage of the solar PV generated energy absorbed locally increased to 91.3% with the percentage of energy supplied by the utility reducing to 53.3%. This translated to an energy saving of approximately 20 kWh per day, this is equal to \$ 3.1 per day based on a tariff of \$ 0.15 per kWh.

In the second scenario (laundry day), the weather status was also classified as "clear skies". The results were similar to the non-laundry day scenario with the exception of the increased percentage of the utility supplied energy (8.81 kWh). The percentage of the solar PV generated energy absorbed locally further increased to 96.6% with the percentage of energy supplied by utility totalling to 53.25%. This translated to an energy saving of approximately 18 kWh per day or \$ 2.76.

CONCLUSION

In this research, a new intelligent energy management system was developed for grid tie residential PV systems. This system was designed in a way that it optimised the utilisation of energy from both the regular electricity grid and the PV system using the historical energy consumption data and the forecasted weather information to enable effective planning of the usage of energy generated from the PV system.

In conclusion, it was observed that the EMS operating alongside a residential PV system increases the local energy consumption percentage by 15-20% when compared to a PV system with no EMS. This translates to a daily energy saving in the range of $ 2.71 to $ 3.1 which makes this EMS a feasible solution to implement along with a residential PV system.

ACKNOWLEDGEMENT

This material is based on research/work supported wholly / in part by the National Research Foundation (NRF) of South Africa. The research findings are that of the authors and not that of the NRF.

REFERENCES

[1] Q. Jiang, M. Xue and G. Geng, “Energy Management of Microgrid in Grid-Connected and Stand-Alone Modes,” *IEEE Transactions on Power Systems,* vol. 28, no. 3, pp. 3380-3389, 2013.

[2] D. Robinson, “Microgrids for Energy Reliability,” *ASHRAE Journal,* vol. 55, no. 11, pp. B14 - B17, 2013.

[3] M. Mikati and M. Santos, “Electric grid dependence on the configuration of a small-scale wind and solar power hybrid system,” *Renewable Energy,* vol. 57, pp. 587-593, 2013.

[4] S. Ramakrishnan and S. Ramakrishnan, “WoT (Web of Things) for Energy Management in a Smart Grid-Connected Home,” *Issues in Informing Science and Information Technology,* vol. 10, pp. 461 - 472, 2013.

[5] M. Schulze and P. Del Granado, “Implementation of feed-in tariffs into multi-energy systems,” *International Journal of Electrical Power and Energy Systems Engineering,* vol. 2, p. 85, 2010.

[6] Eskom , “Tariffs and Charges 2015/2016,” 1 March 2015. [Online]. Available: http://www.eskom.co.za/CustomerCare/TariffsAndCharges/WhatsNew/Documents/Tariff%20brochure%20v9%20lowres.pdf. [Accessed 1 November 2015].

[7] Eskom Newsdesk, “Small and Micro Generation (SMG) Bulletin 1,” 1 September 2015. [Online]. Available: www.eskom.co.za/Whatweredoing/Documents/SMG_Bulletin1.pdf. [Accessed 1 November 2015].

[8] G. M. Bokanga, A. K. Raji and M. T. E. Kahn, “Design of a low voltage DC microgrid system for rural electrification in South Africa,” *Journal of Energy in Southern Africa,* vol. 25, no. 2, p. 9, 2014.